

On a semi-explicit fourth-order vector compact scheme for the multidimensional acoustic wave equation

Alexander Zlotnik^{a,*}, Timofey Lomonosov^a

^a*Department of Mathematics, Higher School of Economics University, Pokrovskii bd. 11, 109028 Moscow, Russia*

Abstract

We deal with an initial-boundary value problem for the multidimensional acoustic wave equation, with the variable speed of sound. For a three-level semi-explicit in time higher-order vector compact scheme, we prove stability and derive 4th order error bound in the enlarged energy norm. This scheme is three-point in each spatial direction, and it exploits additional sought functions which approximate 2nd order non-mixed spatial derivatives of the solution to the equation. At the first time level, a similar two-level in time scheme is applied, with no derivatives of the data. No iterations are required to implement the scheme. We also present results of various 3D numerical experiments that demonstrate a very high accuracy of the scheme for smooth data, its advantages in the error behavior over the classical explicit 2nd order scheme for nonsmooth data as well and an example of the wave in a layered medium initiated by the Ricker-type wavelet source function.

Keywords: acoustic wave equation, semi-explicit vector scheme, higher-order compact scheme, conditional stability, error bound

AMS Subject Classification: 65M06, 65M12, 65M15.

1. Introduction

This paper continues a study of the semi-explicit in time fourth-order vector compact scheme for the multidimensional acoustic wave equation, with the variable speed of sound, that has recently been constructed and investigated in [28, 34]. A nonstandard element of the scheme is the use of additional sought functions that approximate the 2nd order nonmixed spatial derivatives of the solution; that element leads to a simple and direct implementation of the scheme. Its conditional stability in the strong energy norm and the corresponding error bound of the order 3.5 have been proved in [34]. For the wave equation (having constant coefficients), stability in the standard energy norm and the corresponding 4th order error bound have been proved as well, but the argument is not extended to the case of variable coefficients where the 4th order bound has not been proved.

In this paper, we apply another approach based on a theorem of stability in an enlarged weak energy norm for an abstract three-level method together with symmetrization of the scheme being studied. This makes it possible to prove the expected stability in the enlarged (standard) energy norm and the corresponding 4th order error bound. Also, in addition to 2D numerical experiments in [34], we accomplish new 3D ones. First, we show very small errors and their 4th order behavior for smooth travelling wave-type solutions. Second, we demonstrate essential advantages in error and its convergence rates in the mesh L^2 , H^1 and energy norms of the present scheme over the classical explicit 2nd order scheme in the case of nonsmooth data as well. Such important effect is observed namely in the hyperbolic case, and not in the elliptic or parabolic ones. Note that, in 1D case, the practical convergence rates in the case of nonsmooth data were studied for some

*Corresponding author

Email addresses: azlotnik@hse.ru (Alexander Zlotnik), tlomonosov@hse.ru (Timofey Lomonosov)

2nd and 4th order schemes in [32, 33]. Finally, we give an example of a wave propagation in a three-layer medium, with a piecewise constant speed of sound, initiated by a smoothed Ricker-type wavelet source.

The semi-explicit vector compact scheme was originally suggested for the 2D wave equation in [13]. Its generalization to the n -dimensional wave and acoustic wave equations, $n \geq 1$, has been given in [28] (including the case of nonuniform meshes in space and time). Recall that the case $n \geq 4$ is of interest in theoretical physics, for example, see [12]. The cases of the 3D wave and acoustic wave equations have been also considered in [14], where another spatial discretization in the latter case has been suggested; the case of mildly nonlinear wave equation has been covered as well. Notice that a rigorous justification of the last mentioned discretization is absent and seems to be a technically complicated task.

We should notice that other compact 4th-order schemes were developed much earlier, and a vast literature is devoted to them. The most standard of them were derived based mainly on an analysis and approximation of the leading term of the approximation error of second order schemes, in particular, see [4, 21, 23, 25, 33, 31], etc. For the acoustic wave equation, rigorous stability theorems and corresponding 4th order error bounds for schemes of such type have recently been proved in [31]. But such schemes are implicit, and their effective implementation for the acoustic wave equation needs application of iterative methods that entails increasing of computational costs.

A natural development of such compact schemes led to their various alternating-direction implicit (ADI) versions, see such 4th order schemes, in particular, in [7, 10, 11, 17, 18, 26, 33] and, in the case of the acoustic wave equation, in [16, 19, 30]. To implement them, one needs to solve only 1D systems of linear algebraic equations with tridiagonal matrices; thus, no iterative methods are required, that is essentially simpler. But, for the acoustic wave equation, rigorous stability theorems and corresponding 4th order error bounds face essential difficulties and are not available up to the moment. Note that implicitness and conditional stability are immanent to all three types of compact 4th order schemes listed above.

We also mention that, for the wave-type equations, there exist a lot of quite different higher-order methods, in particular, see [1, 5, 6, 8, 9, 15, 24] and references therein.

Content of the paper is as follows. In Section 2, we state the initial-boundary value problem (IBVP) for the acoustic wave equation, with nonhomogeneous Dirichlet boundary conditions, briefly recall how to construct the semi-explicit vector compact scheme to solve it and discuss its fast implementation. For this scheme, in the next Section 3, a stability theorem in the enlarged energy norm and the corresponding theorem on the 4th order error bound are derived. In the last Section 4, we give results of various 3D numerical experiments demonstrating the very high accuracy of the scheme for smooth data, its advantages in the error behavior over the classical explicit 2nd order scheme for nonsmooth data as well and an example of the wave in a layered medium initiated by the Ricker-type wavelet source function.

2. The multidimensional acoustic wave equation and a semi-explicit 4th-order vector compact scheme to solve it

In this paper, we treat an IBVP (initial-boundary value problem) for the n -dimensional acoustic wave equation

$$\rho(x)\partial_t^2 u(x, t) - Lu(x, t) = f(x, t), \quad L := a_1^2 \partial_1^2 + \dots + a_n^2 \partial_n^2, \quad \text{in } Q_T = \Omega \times (0, T); \quad (2.1)$$

$$u|_{\Gamma_T} = g(x, t); \quad u|_{t=0} = u_0(x), \quad \partial_t u|_{t=0} = u_1(x), \quad x \in \Omega = (0, X_1) \times \dots \times (0, X_n), \quad (2.2)$$

where the nonhomogeneous Dirichlet boundary condition is used. Here $0 < \underline{\rho} \leq \rho(x) \leq \bar{\rho}$ and $a_1 > 0, \dots, a_n > 0$ are constants (they are taken different like in [33, 31, 34]), $x = (x_1, \dots, x_n)$, $n \geq 1$. In addition, $\partial\Omega$ and $\Gamma_T = \partial\Omega \times (0, T)$ are the boundary of Ω and the lateral surface of Q_T , respectively. Let $a_{\max} := \max_{1 \leq k \leq n} a_k$. We first assume that ρ and u are smooth (the nonsmooth examples will be taken in Section 4).

We introduce the uniform mesh $\bar{\omega}_{h_t}$ with the nodes $t_m = mh_t$, $0 \leq m \leq M$ and the step $h_t = T/M > 0$ on $[0, T]$; here $M \geq 2$. Let $\omega_{h_t} = \{t_m\}_{m=1}^{M-1}$. We define the mesh averages including the Numerov one,

difference operators and the summation operator in time levels with the variable upper limit

$$\bar{s}_t y = \frac{1}{2}(\tilde{y} + y), \quad s_{tN} y = \frac{1}{12}(\tilde{y} + 10y + \hat{y}), \quad \bar{\delta}_t y = \frac{y - \tilde{y}}{h_t}, \quad \delta_t y = \frac{\hat{y} - y}{h_t}, \quad \Lambda_t y = \delta_t \bar{\delta}_t y = \frac{\hat{y} - 2y + \tilde{y}}{h_t^2},$$

$$I_{h_t}^m y = h_t \sum_{l=1}^m y^l \quad \text{for } 1 \leq m \leq M, \quad I_{h_t}^0 y = 0.$$

where $y^m = y(t_m)$, $\tilde{y}^m = y^{m-1}$ and $\hat{y}^m = y^{m+1}$.

We introduce the uniform mesh $\bar{\omega}_{hk}$ with the nodes $x_{ki} = ih_k$, $0 \leq i \leq N_k$, with the step $h_k = X_k/N_k$ in x_k . Denote by $\omega_{hk} = \{x_{ki}\}_{i=1}^{N_k-1}$ its internal part. We define the difference operator and the Numerov average in x_k :

$$(\Lambda_k w)_i := \frac{1}{h_k^2}(w_{i+1} - 2w_i + w_{i-1}), \quad s_{kN} w_i := \frac{1}{12}(w_{i-1} + 10w_i + w_{i+1}) = (I + \frac{1}{12}h_k^2 \Lambda_k)w_i \quad (2.3)$$

on ω_{hk} , where $w_i = w(x_{ki})$.

Further, we introduce the rectangular mesh $\bar{\omega}_h = \bar{\omega}_{h_1} \times \dots \times \bar{\omega}_{h_n}$ in $\bar{\Omega}$, where $h = (h_1, \dots, h_n)$. Let $\omega_h = \omega_{h_1} \times \dots \times \omega_{h_n}$ and $\partial\omega_h = \bar{\omega}_h \setminus \omega_h$. We introduce the meshes $\omega_{\mathbf{h}} := \omega_h \times \omega_{h_t}$ in Q_T and $\partial\omega_{\mathbf{h}} = \partial\omega_h \times \{t_m\}_{m=1}^M$ on $\bar{\Gamma}_T$, with $\mathbf{h} = (h, h_t)$.

We denote by H_h a Euclidean space of functions, with the inner product $(v, w)_h$ and norm $\|w\|_h = (w, w)_h^{1/2}$. For a linear operator C_h acting in H_h , we denote by $\|C_h\|$ its norm. Any such $C_h = C_h^* > 0$ generates the norm $\|w\|_{C_h} := (C_h w, w)_h^{1/2} = \|C_h^{1/2} w\|_h$ in H_h . Let I be the unit operator.

Unless otherwise stated, below H_h is the space of functions given on $\bar{\omega}_h$ and equal 0 on $\partial\omega_h$, with the L^2 -type inner product

$$(v, w)_h = h_1 \dots h_n \sum_{x_i \in \omega_h} v(x_i)w(x_i), \quad x_i = (i_1 h_1, \dots, i_n h_n), \quad \mathbf{i} = (i_1, \dots, i_n).$$

We define the simplest difference approximation $L_h := a_1^2 \Lambda_1 + \dots + a_n^2 \Lambda_n$ of L . It is well-known that

$$\frac{4}{X_k^2} I < -\Lambda_k = -\Lambda_k^* < \frac{4}{h_k^2} I, \quad \frac{2}{3} I < s_{kN} = s_{kN}^* < I, \quad (2.4)$$

$$0 < -L_h = -L_h^* < 4\left(\frac{a_1^2}{h_1^2} + \dots + \frac{a_n^2}{h_n^2}\right) I. \quad (2.5)$$

Hereafter all the operator inequalities concern self-adjoint operators in H_h .

For completeness, we briefly recall the derivation of the method under consideration. First we replace the acoustic wave equation (2.1) with a system of equations with second order partial derivative either in t , or in x_k :

$$\rho(x) \partial_t^2 u(x, t) - (a_1^2 u_{11}(x, t) + \dots + a_n^2 u_{nn}(x, t)) = f(x, t) \quad \text{in } Q_T,$$

$$u_{kk}(x, t) := \partial_k^2 u(x, t), \quad 1 \leq k \leq n, \quad \text{in } Q_T, \quad (2.6)$$

where u_{11}, \dots, u_{nn} are the additional functions to seek. Differentiating Eq. (2.1), we get

$$\rho \partial_t^4 u = \partial_t^2 (Lu + f) = L\left[\frac{1}{\rho}(Lu + f)\right] + \partial_t^2 f. \quad (2.7)$$

Thus, we can sequentially write

$$\begin{aligned} \rho \Lambda_t u &= \rho \partial_t^2 u + \frac{1}{12} h_t^2 \rho \partial_t^4 u + \mathcal{O}(h_t^4) \\ &= (\rho I + \frac{1}{12} h_t^2 L) \left(\frac{1}{\rho} Lu \right) + f + \frac{1}{12} h_t^2 (\partial_t^2 f + L \frac{f}{\rho}) + \mathcal{O}(h_t^4) \\ &= (\rho I + \frac{1}{12} h_t^2 L_h) \frac{1}{\rho} (a_1^2 u_{11} + \dots + a_n^2 u_{nn}) + f_{\mathbf{h}} + \mathcal{O}(|\mathbf{h}|^4), \quad \text{with } f_{\mathbf{h}} := f + \frac{1}{12} h_t^2 (\Lambda_t f + L_h \frac{f}{\rho}). \end{aligned} \quad (2.8)$$

Next, since the auxiliary equation (2.6) is an ordinary differential equation in x_k , its well-known Numerov approximation leads to the formula

$$s_{kN}u_{kk} - \Lambda_k u = \mathcal{O}(h_k^4) \quad \text{on } \omega_{\mathbf{h}}, \quad 1 \leq k \leq n. \quad (2.9)$$

One can omit the residues in the derived expansions (2.8)-(2.9) and thus obtain *the three-level semi-explicit in time vector compact scheme*

$$\rho \Lambda_t v - \left(\rho I + \frac{1}{12} h_t^2 L_h\right) \frac{1}{\rho} (a_1^2 v_{11} + \dots + a_n^2 v_{nn}) = f_{\mathbf{h}} \quad \text{on } \omega_{\mathbf{h}}, \quad (2.10)$$

$$s_{kN}v_{kk} = \Lambda_k v \quad \text{on } \omega_{\mathbf{h}}, \quad 1 \leq k \leq n, \quad (2.11)$$

with the main sought function $v \approx u$ given on $\bar{\omega}_h \times \bar{\omega}_{h_t}$ and additional ones $v_{11} \approx u_{11}, \dots, v_{nn} \approx u_{nn}$ given on $\bar{\omega}_h \times \omega_{h_t}$. The collection of these functions constitutes the sought vector-function.

The mesh boundary conditions

$$v|_{\partial\omega_{\mathbf{h}}} = g, \quad a_k^2 v_{kk}|_{\partial\omega_{\mathbf{h}}} = g_k, \quad 1 \leq k \leq n, \quad (2.12)$$

are added according to the boundary condition $u|_{\Gamma_T} = g$ and the acoustic wave equation in \bar{Q}_T :

$$g_k = \rho \partial_t^2 g - \sum_{1 \leq l \leq n, l \neq k} a_l^2 \partial_l^2 g - f \quad \text{for } x_k = 0, X_k,$$

$$g_k = a_k^2 \partial_k^2 g \quad \text{for } x_l = 0, X_l, \quad 1 \leq l \leq n, \quad l \neq k,$$

on parts of Γ_T . In the simplest case $g = 0$, the right-hand side of the former formula equals $-f$ and of the latter one is zero.

In addition, the function v^m should be found at the first time level $m = 1$ with the 4th order of accuracy. This is often done explicitly by using Taylor's formula and the wave equation, for example, see [4, 11, 13, 14, 25]. These cumbersome formulas use higher-order derivatives of u_0 and u_1 ; they cannot be used when u_0 and u_1 are nonsmooth. Instead, like in [27, 31, 34], we apply an equation for v^1 similar to the above main equations (2.10)-(2.11) of the scheme:

$$\rho(\delta_t v)^0 = \frac{1}{2} h_t (\rho I + \frac{1}{12} h_t^2 L_h) \frac{1}{\rho} (a_1^2 v_{11}^0 + \dots + a_n^2 v_{nn}^0) + u_{1\mathbf{h}} + \frac{1}{2} h_t f_{\mathbf{h}}^0 \quad \text{on } \omega_{\mathbf{h}}, \quad (2.13)$$

$$s_{kN}v_{kk}^0 = \Lambda_k v^0 \quad \text{on } \omega_{\mathbf{h}}, \quad 1 \leq k \leq n, \quad (2.14)$$

with the specific $u_{1\mathbf{h}} \approx \rho u_1$ and $f_{\mathbf{h}}^0 \approx f_0 = f|_{t=0}$ such that

$$u_{1\mathbf{h}} := (\rho I + \frac{1}{6} h_t^2 L_h) u_1, \quad f_{\mathbf{h}}^0 := f_{dh_t}^{(0)} + \frac{1}{12} h_t^2 L_h \frac{f_0}{\rho} \quad \text{on } \omega_{\mathbf{h}}, \quad (2.15)$$

$$f_{dh_t}^{(0)} = \frac{7}{12} f^0 + \frac{1}{2} f^1 - \frac{1}{12} f^2 \quad \text{or} \quad f_{dh_t}^{(0)} = \frac{1}{3} f^0 + \frac{2}{3} f^{1/2}, \quad \text{with } f^{1/2} := f|_{t=h_t/2}. \quad (2.16)$$

The values of v_{kk}^0 on $\partial\omega_{\mathbf{h}}$ can be taken as in (2.12) (or, for smooth u_0 , using the values of $\partial_k^2 u_0$ on $\partial\Omega$). Due to such formulas, the approximation error of Eq. (2.13) has the 4th order

$$\hat{\psi}^0 := \rho(\delta_t u)^0 - \frac{1}{2} h_t (\rho I + \frac{1}{12} h_t^2 L_h) \frac{1}{\rho} (a_1^2 u_{110} + \dots + a_n^2 u_{nn0}) - u_{1\mathbf{h}} - \frac{1}{2} h_t f_{\mathbf{h}}^0 = \mathcal{O}(|\mathbf{h}|^4) \quad \text{on } \omega_{\mathbf{h}}, \quad (2.17)$$

see [34]. Hereafter $y_0 := y|_{t=0}$ for any t -dependent function y .

In numerical experiments below, the second (two-level) formula in (2.16) together with more suitable forms of Eqs. (2.10) and (2.13) are applied

$$\rho \Lambda_t v = \left(\rho I + \frac{1}{12} h_t^2 L_h\right) \frac{1}{\rho} (a_1^2 v_{11} + \dots + a_n^2 v_{nn} + f) + \frac{1}{12} h_t^2 \Lambda_t f \quad \text{on } \omega_{\mathbf{h}},$$

$$\rho(\delta_t v)^0 = \frac{1}{2} h_t \left\{ \rho(a_1^2 v_{11}^0 + \dots + a_n^2 v_{nn}^0) + f_{dh_t}^{(0)} + \frac{1}{12} h_t^2 L_h \left[\frac{1}{\rho} (a_1^2 v_{11}^0 + \dots + a_n^2 v_{nn}^0 + f^0) \right] \right\} + u_{1\mathbf{h}} \quad \text{on } \omega_{\mathbf{h}}.$$

The described scheme is semi-explicit in time. The function v^{m+1} is found explicitly on $\omega_{\mathbf{h}}$ from (2.10) for $1 \leq m \leq M-1$ or (2.13) for $m = 0$ when the auxiliary functions $v_{11}^m, \dots, v_{nn}^m$ are known on $\bar{\omega}_h$. These functions are computed from the simple 1D three-point difference equations (2.11) for $1 \leq m \leq M-1$ or (2.14) for $m = 0$ together with the boundary conditions from (2.12) when v^m is known. Thus there exists an analogy in implementation with the ADI methods, for example, see [20]. On the other hand, the functions $v_{11}^m, \dots, v_{nn}^m$ are independent and allow us multithreaded computation (that we exploit in Section 4), and we only need to store their weighted sum in order to save computer memory.

3. Stability and the 4th order error bound for the semi-explicit vector compact scheme

We first prove an auxiliary general result.

Lemma 3.1. *Consider an abstract three-level scheme*

$$B_h \Lambda_t v + A_h v = \varphi \quad \text{in } H_h \quad \text{on } \omega_{h_t}, \quad (3.1)$$

$$B_h(\delta_t v)^0 + \frac{1}{2} h_t A_h v^0 = u^{(1)} + \frac{1}{2} h_t \varphi^0 \quad \text{in } H_h \quad (3.2)$$

for a function $v: \bar{\omega}_{h_t} \rightarrow H_h$. Here $B_h = B_h^* > 0$ and $A_h = A_h^* > 0$ are operators acting in a Euclidean space H_h such that

$$\frac{1}{4} h_t^2 A_h \leq (1 - \varepsilon_0^2) B_h \quad \text{for some } 0 < \varepsilon_0 < 1. \quad (3.3)$$

Then the following stability bounds hold

$$\max_{0 \leq m \leq M} \max \{ \varepsilon_0 \|v^m\|_{B_h}, \|I_{h_t}^m \bar{s}_t v\|_{A_h} \} \leq \|v^0\|_{B_h} + 2 \|A_h^{-1/2} u^{(1)}\|_h + 2 \|A_h^{-1/2} \varphi\|_{\tilde{L}_{h_t}^1(H_h)}, \quad (3.4)$$

$$\varepsilon_0 \max_{1 \leq m \leq M} \|A_h^{-1/2} B_h \delta_t v\|_h \leq (1 + \varepsilon_0) \|v^0\|_{B_h} + (3 + 2\varepsilon_0) (\|A_h^{-1/2} u^{(1)}\|_h + \|A_h^{-1/2} \varphi\|_{\tilde{L}_{h_t}^1(H_h)}). \quad (3.5)$$

Here, we use the norm $\|y\|_{\tilde{L}_{h_t}^1(H_h)} := \frac{1}{2} h_t \|y^0\|_h + h_t \sum_{m=1}^{M-1} \|y^m\|_h$ for functions $y: \{t_m\}_{m=0}^{M-1} \rightarrow H_h$.

Proof. Bound (3.4) follows from the known bound in the weak energy norm

$$\begin{aligned} & \max_{0 \leq m \leq M} \max \{ [\|v^m\|_{B_h}^2 - \frac{1}{4} h_t^2 \|v^m\|_{A_h}^2]^{1/2}, \|I_{h_t}^m \bar{s}_t v\|_{A_h} \} \\ & \leq [\|v^0\|_{B_h}^2 - \frac{1}{4} h_t^2 \|v^0\|_{A_h}^2]^{1/2} + 2 \|A_h^{-1/2} u^{(1)}\|_h + 2 \|A_h^{-1/2} \varphi\|_{\tilde{L}_{h_t}^1(H_h)}, \end{aligned}$$

see [33, Theorem 1] and [29, Theorem 2] (for the weight $\sigma = 0$), and from condition (3.3).

To derive bound (3.5), we apply the operator I_{h_t} to Eq. (3.1) and get

$$B_h(\delta_t v^m - \delta_t v^0) + A_h I_{h_t}^m v = I_{h_t}^m \varphi, \quad 0 \leq m \leq M-1.$$

Due to the initial condition (3.2) and the elementary formula

$$\frac{1}{2} h_t v^0 + I_{h_t}^m v = I_{h_t}^m \bar{s}_t v + \frac{1}{2} h_t v^m, \quad 0 \leq m \leq M, \quad (3.6)$$

we further obtain

$$B_h \delta_t v^m = -A_h (I_{h_t}^m \bar{s}_t v + \frac{1}{2} h_t v^m) + u^{(1)} + \frac{1}{2} h_t \varphi^0 + I_{h_t}^m \varphi, \quad 0 \leq m \leq M-1.$$

Next, we apply the operator $A_h^{-1/2}$ to both sides of this equality, take the norm in H_h and, using condition (3.3), derive

$$\begin{aligned} \|A_h^{-1/2} B_h \delta_t v^{m+1}\|_h & \leq \|I_{h_t}^m \bar{s}_t v\|_{A_h} + \frac{1}{2} h_t \|v^m\|_{A_h} + \|A_h^{-1/2} u^{(1)}\|_h + \frac{1}{2} h_t \|A_h^{-1/2} \varphi^0\|_h + \|I_{h_t}^m \|A_h^{-1/2} \varphi\|_h \\ & \leq (1 + \varepsilon_0^{-1}) \max \{ \varepsilon_0 \|v^m\|_{B_h}, \|I_{h_t}^m \bar{s}_t v\|_{A_h} \} + \|A_h^{-1/2} u^{(1)}\|_h + \|A_h^{-1/2} \varphi\|_{\tilde{L}_{h_t}^1(H_h)}. \end{aligned}$$

Now the first bound of this Lemma implies the second one. \square

Remark 3.1. *Due to formula (3.6) and condition (3.3), we obtain*

$$\|I_{h_t}^m v\|_{A_h} \leq \frac{1}{2} h_t \|v^0\|_{A_h} + \|I_{h_t}^m \bar{s}_t v\|_{A_h} + \frac{1}{2} h_t \|v^m\|_{A_h} \leq \|v^0\|_{B_h} + \|I_{h_t}^m \bar{s}_t v\|_{A_h} + \|v^m\|_{B_h}, \quad 0 \leq m \leq M.$$

Thus, an additional bound holds

$$\varepsilon_0 \max_{0 \leq m \leq M} \|I_{h_t}^m v\|_{A_h} \leq (2 + 2\varepsilon_0) (\|v^0\|_{B_h} + \|A_h^{-1/2} u^{(1)}\|_h + \|A_h^{-1/2} \varphi\|_{\tilde{L}_{h_t}^1(H_h)}).$$

We consider the inhomogeneous version of Eqs. (2.11) and (2.14):

$$s_{kN}v_{kk}^m = \Lambda_k v^m + b_k^m \quad \text{on } \omega_h, \quad 0 \leq m \leq M-1, \quad 1 \leq k \leq n, \quad (3.7)$$

with the given functions b_1, \dots, b_n . In practical computations, one never has $b_1 = \dots = b_n = 0$ due to the presence of the round-off errors. Therefore, an impact of b_1, \dots, b_n on v has to be studied. Importantly, one must do that to prove error bounds for the scheme.

We define the following two self-adjoint operators in H_h :

$$E_h := -(a_1^2 s_{1N}^{-1} \Lambda_1 + \dots + a_n^2 s_{nN}^{-1} \Lambda_n), \quad I_{\rho\mathbf{h}} := \frac{1}{\rho} I + \frac{1}{12} h_t^2 \left(\frac{1}{\rho} L_h \right) \frac{1}{\rho} I.$$

The second inequality (2.4) can be rewritten as $I < s_{1N}^{-1} < (3/2)I$ and thus $-L_h < E_h < -(3/2)L_h$. Clearly also $I_{\rho\mathbf{h}} = I_{\rho\mathbf{h}}^* < \rho^{-1}I \leq \underline{\rho}^{-1}I$.

We introduce the first CFL-type condition on h_t and h_1, \dots, h_n :

$$\frac{1}{3} h_t^2 \left(\frac{a_1^2}{h_1^2} + \dots + \frac{a_n^2}{h_n^2} \right) \leq (1 - \varepsilon) \underline{\rho} \quad \text{for some } 0 \leq \varepsilon < 1. \quad (3.8)$$

Then with the help of inequality (2.5) we have

$$-\left(\frac{1}{12} h_t^2 \left(\frac{1}{\rho} L_h \right) \frac{w}{\rho}, w \right)_h = -\frac{1}{12} h_t^2 \left(L_h \frac{w}{\rho}, \frac{w}{\rho} \right)_h < (1 - \varepsilon) \underline{\rho} \left(\frac{w}{\rho}, \frac{w}{\rho} \right)_h \leq (1 - \varepsilon) \left(\frac{1}{\rho} w, w \right)_h \quad \text{for any } w \in H_h$$

and, consequently, we can also bound $I_{\rho\mathbf{h}}$ from below and get the two-sided bounds

$$\varepsilon \frac{1}{\rho} I \leq \varepsilon \frac{1}{\rho} I < I_{\rho\mathbf{h}} < \frac{1}{\rho} I \leq \frac{1}{\underline{\rho}} I. \quad (3.9)$$

For $0 < \varepsilon < 1$, these bounds are equivalent to the following ones

$$\underline{\rho} I \leq \rho I < I_{\rho\mathbf{h}}^{-1} < \varepsilon^{-1} \rho I \leq \varepsilon^{-1} \bar{\rho} I. \quad (3.10)$$

The new stability result on the semi-explicit vector compact scheme is as follows.

Theorem 3.1. *Assume that the stability conditions (3.8) and*

$$\frac{1}{4} h_t^2 E_h \leq (1 - \varepsilon_0^2) \underline{\rho} I \quad \text{for some } 0 < \varepsilon_0 < 1 \quad (3.11)$$

are valid, and $g = g_1 = \dots = g_n = 0$ in the boundary conditions (2.12). Then the following stability bounds hold

$$\max_{0 \leq m \leq M} \max \left\{ \varepsilon_0 \|v^m\|_{E_h}, \|I_{\rho\mathbf{h}}^m \bar{s}_t E_h v\|_{I_{\rho\mathbf{h}}} \right\} \leq \|v^0\|_{E_h} + 2 \left\| \frac{1}{\rho} u_{1\mathbf{h}} \right\|_{I_{\rho\mathbf{h}}^{-1}} + 2 \left\| I_{\rho\mathbf{h}}^{-1/2} \left[\frac{1}{\rho} (f_{\mathbf{h}} + \beta_{\mathbf{h}}) \right] \right\|_{\bar{L}_{h_t}^1(H_h)}, \quad (3.12)$$

$$\varepsilon_0 \max_{1 \leq m \leq M} \|\bar{\delta}_t v^m\|_{I_{\rho\mathbf{h}}^{-1}} \leq (1 + \varepsilon_0) \|v^0\|_{E_h} + (3 + 2\varepsilon_0) \left(\left\| \frac{1}{\rho} u_{1\mathbf{h}} \right\|_{I_{\rho\mathbf{h}}^{-1}} + \left\| I_{\rho\mathbf{h}}^{-1/2} \left[\frac{1}{\rho} (f_{\mathbf{h}} + \beta_{\mathbf{h}}) \right] \right\|_{\bar{L}_{h_t}^1(H_h)} \right), \quad (3.13)$$

for any functions $f_{\mathbf{h}}, b_1, \dots, b_n$: $\{t_m\}_{m=0}^{M-1} \rightarrow H_h$ and $v^0, u_{1\mathbf{h}} \in H_h$ (thus, $f_{\mathbf{h}}$ and $u_{1\mathbf{h}}$ are not only those specific functions defined (2.15)-(2.16)) and

$$\beta_{\mathbf{h}}^m := \left(\rho I + \frac{1}{12} h_t^2 L_h \right) \frac{1}{\rho} (a_1^2 s_{1N}^{-1} b_1^m + \dots + a_n^2 s_{nN}^{-1} b_n^m) \quad \text{in } H_h, \quad 0 \leq m \leq M-1. \quad (3.14)$$

Proof. Since $g = g_1 = \dots = g_n = 0$, clearly v : $\bar{\omega}_{h_t} \rightarrow H_h$ and v_{kk} : $\{t_m\}_{m=0}^{M-1} \rightarrow H_h$, $1 \leq k \leq n$. Acting as in [34], we can express v_{kk} from Eq. (3.7):

$$v_{kk}^m = s_{kN}^{-1} (\Lambda_k v^m + b_k^m) \quad \text{in } H_h, \quad 1 \leq k \leq n, \quad 0 \leq m \leq M-1. \quad (3.15)$$

Using these expressions in Eqs. (2.10) and (2.13) leads to the equations for v only:

$$\begin{aligned} \rho \Lambda_t v^m + \left(\rho I + \frac{1}{12} h_t^2 L_h \right) \frac{1}{\rho} E_h v^m &= f_{\mathbf{h}}^m + \beta_{\mathbf{h}}^m \quad \text{in } H_h, \quad 1 \leq m \leq M-1, \\ \rho (\delta_t v)^0 + \frac{1}{2} h_t \left(\rho I + \frac{1}{12} h_t^2 L_h \right) \frac{1}{\rho} E_h v^0 &= u_{1\mathbf{h}} + \frac{1}{2} h_t (f_{\mathbf{h}}^0 + \beta_{\mathbf{h}}^0) \quad \text{in } H_h; \end{aligned}$$

recall that $\beta_{\mathbf{h}}$ has been introduced in (3.14).

Importantly, both the equations can be symmetrized by applying the operator $E_h(\rho^{-1}I)$ to them

$$E_h \Lambda_t v^m + E_h I_{\rho \mathbf{h}} E_h v^m = E_h \left(\frac{1}{\rho} (f_{\mathbf{h}} + \beta_{\mathbf{h}})^m \right) \quad \text{in } H_h, \quad 1 \leq m \leq M-1, \quad (3.16)$$

$$E_h (\delta_t v)^0 + \frac{1}{2} h_t E_h I_{\rho \mathbf{h}} E_h v^0 = E_h \left(\frac{1}{\rho} u_{1\mathbf{h}} \right) + \frac{1}{2} h_t E_h \left(\frac{1}{\rho} (f_{\mathbf{h}}^0 + \beta_{\mathbf{h}}^0) \right) \quad \text{in } H_h. \quad (3.17)$$

Here $E_h I_{\rho \mathbf{h}} E_h = (E_h I_{\rho \mathbf{h}} E_h)^* > 0$ under condition (3.8) due to inequalities (3.9), therefore, these equations can be treated as a particular case of scheme (3.1)-(3.2) for $B_h = E_h$ and $A_h = E_h I_{\rho \mathbf{h}} E_h$.

Now the general stability condition (3.3) looks as

$$\frac{1}{4} h_t^2 E_h I_{\rho \mathbf{h}} E_h \leq (1 - \varepsilon_0^2) E_h \quad \text{for some } 0 < \varepsilon_0 < 1.$$

Recall that $I_{\rho \mathbf{h}} < \underline{\rho}^{-1} I$, thus the last condition follows from $(1/4) h_t^2 E_h^2 \leq (1 - \varepsilon_0^2) \underline{\rho} E_h$ or, equivalently, from (3.11).

Next, for any $w \in H_h$, we have

$$\begin{aligned} \|w\|_{A_h}^2 &= (E_h I_{\rho \mathbf{h}} E_h w, w)_h = \|E_h w\|_{I_{\rho \mathbf{h}}}^2, \\ \|A_h^{-1/2} B_h w\|_h^2 &= (A_h^{-1} B_h w, B_h w)_h = ((E_h I_{\rho \mathbf{h}} E_h)^{-1} E_h w, E_h w)_h = (I_{\rho \mathbf{h}}^{-1} w, w)_h = \|w\|_{I_{\rho \mathbf{h}}^{-1}}^2. \end{aligned}$$

Consequently, the general stability bounds (3.4)-(3.5) take the form of the stated bounds (3.12)-(3.13). \square

Since $E_h < \frac{3}{2}(-L_h)$ in H_h , both the stability conditions (3.8) and (3.11) follow from the inequality

$$h_t^2 \left(\frac{a_1^2}{h_1^2} + \dots + \frac{a_n^2}{h_n^2} \right) \leq \min\{3(1 - \varepsilon), \frac{2}{3}(1 - \varepsilon_0^2)\} \underline{\rho}.$$

The right-hand sides of bounds (3.12)-(3.13) can be simplified. Due to the formula $\rho^{-1} \beta_{\mathbf{h}} = I_{\rho \mathbf{h}} (a_1^2 s_{1N}^{-1} b_1 + \dots + a_n^2 s_{nN}^{-1} b_n)$ and the operator inequalities (3.9), (3.10) and $s_{kN}^{-1} \leq (3/2)I$, for $0 < \varepsilon < 1$, we get

$$\|I_{\rho \mathbf{h}}^{-1/2} \left[\frac{1}{\rho} (f_{\mathbf{h}} + \beta_{\mathbf{h}}) \right]\|_{\tilde{L}_{h_t}^1(H_h)} \leq \varepsilon^{-1/2} \left\| \frac{f_{\mathbf{h}}}{\sqrt{\rho}} \right\|_{\tilde{L}_{h_t}^1(H_h)} + \|I_{\rho \mathbf{h}}^{1/2} (a_1^2 s_{1N}^{-1} b_1 + \dots + a_n^2 s_{nN}^{-1} b_n)\|_{\tilde{L}_{h_t}^1(H_h)} \quad (3.18)$$

$$\leq \underline{\rho}^{-1/2} \left(\varepsilon^{-1/2} \|f_{\mathbf{h}}\|_{\tilde{L}_{h_t}^1(H_h)} + \frac{3}{2} a_{\max}^2 \sum_{k=1}^n \|b_k\|_{\tilde{L}_{h_t}^1(H_h)} \right), \quad (3.19)$$

$$\left\| \frac{1}{\rho} u_{1\mathbf{h}} \right\|_{I_{\rho \mathbf{h}}^{-1}} = \|I_{\rho \mathbf{h}}^{-1/2} \left(\frac{1}{\rho} u_{1\mathbf{h}} \right)\|_h \leq (\varepsilon \underline{\rho})^{-1/2} \|u_{1\mathbf{h}}\|_h, \quad \underline{\rho}^{1/2} \|\bar{\delta}_t v^m\|_h \leq \|\bar{\delta}_t v^m\|_{I_{\rho \mathbf{h}}^{-1}}. \quad (3.20)$$

Let $1 \leq k \leq n$. For functions w defined on $\bar{\omega}_{hk}$, we introduce a difference operator and seminorms

$$(\bar{\delta}_k w)_i = \frac{1}{h_k} (w_i - w_{i-1}), \quad 1 \leq i \leq N_k, \quad \|w\|_k = \left(h_k \sum_{i=1}^{N_k-1} w_i^2 \right)^{1/2}, \quad \|w\|_{k*} = \left(h_k \sum_{i=1}^{N_k} w_i^2 \right)^{1/2}.$$

For functions w given on $\bar{\omega}_h$, we have $\|w\|_h = \|\dots\|_w\|_1 \dots\|_n$. Introduce seminorms $\|w\|_{h,k*}$ which defer from $\|w\|_h$ by replacing $\|w\|_k$ with $\|w\|_{k*}$ and then a mesh counterpart of the squared norm in the Sobolev subspace $H_0^1(\Omega)$:

$$\|w\|_{H_h^1}^2 := \|(-L_h)^{1/2} w\|_h^2 = (-L_h w, w)_h = \sum_{k=1}^n a_k^2 \|\bar{\delta}_k w\|_{h,k*}^2.$$

Note the two-sided bounds $\|w\|_{H_h^1}^2 \leq \|w\|_{E_h}^2 \leq \frac{3}{2} \|w\|_{H_h^1}^2$. We also define the mesh energy norm $\|y\|_{\varepsilon_h} := (\|\bar{\delta}_t y\|_h^2 + \|y\|_{H_h^1}^2)^{1/2}$ that is needed in Section 4.

The next theorem states the 4th order error bound in the enlarged mesh energy norm, and it is derived from Theorem 3.1. In this theorem, g and $f|_{\Gamma_T}$ can be arbitrary (not only zero).

Theorem 3.2. *Let the stability conditions (3.8) with $0 < \varepsilon < 1$ and (3.11) hold, and $v^0 = u^0$ on $\bar{\omega}_h$. Then the 4th order error bound in the enlarged mesh energy norm for scheme (2.10)-(2.14) holds*

$$\sqrt{\varepsilon}\varepsilon_0 \max_{1 \leq m \leq M} (\|\bar{\delta}_t(u-v)^m\|_h + \|(u-v)^m\|_{H_h^1} + \sqrt{\varepsilon}\|I_{h_t}^m L_h(u-v)\|_h) = \mathcal{O}(|\mathbf{h}|^4). \quad (3.21)$$

Here and below the $\mathcal{O}(|\mathbf{h}|^4)$ -terms do not depend on ε and ε_0 .

Proof. First, the approximation errors of Eqs. (2.10), (2.11) and (2.14) are expressed by the formulas

$$\begin{aligned} \psi &:= \rho \Lambda_t u - \left(\rho I + \frac{1}{12} h_t^2 L_h\right) \frac{1}{\rho} (a_1^2 u_{11} + \dots + a_n^2 u_{nn}) + f_{\mathbf{h}} \quad \text{on } \omega_{\mathbf{h}}, \\ \psi_{kk} &:= s_{kN} u_{kk} - \Lambda_k u \quad \text{on } \omega_{\mathbf{h}}, \quad \psi_{kk}^0 := s_{kN} \partial_k^2 u_0 - \Lambda_k u_0 \quad \text{on } \omega_h, \quad 1 \leq k \leq n, \end{aligned}$$

whereas the approximation error of Eq. (2.13) has been given by (2.17). According to formulas (2.8), (2.9) and (2.17), all the approximation errors are of the 4th order in the mesh uniform norm

$$\max_{\omega_{\mathbf{h}}} |\psi| + \max_{\omega_{\mathbf{h}}} |\hat{\psi}^0| + \max_{0 \leq m \leq M-1} \max_{\omega_h} (|\psi_{11}^m| + \dots + |\psi_{nn}^m|) = \mathcal{O}(|\mathbf{h}|^4). \quad (3.22)$$

Due to the equations for v and v_{11}, \dots, v_{nn} as well as the definitions of ψ , ψ_{kk} and $\hat{\psi}^0$, the errors $r = u - v$ and $r_{11} = u_{11} - v_{11}, \dots, r_{nn} = u_{nn} - v_{nn}$ satisfy the following system of equations

$$\begin{aligned} \rho \Lambda_t r - \left(\rho I + \frac{1}{12} h_t^2 L_h\right) \frac{1}{\rho} (a_1^2 r_{11} + \dots + a_n^2 r_{nn}) &= \psi \quad \text{on } \omega_{\mathbf{h}}, \\ s_{kN} r_{kk} - \Lambda_k r &= \psi_{kk} \quad \text{on } \omega_{\mathbf{h}}, \quad s_{kN} r_{kk}^0 - \Lambda_k r^0 = \psi_{kk}^0 \quad \text{on } \omega_h, \quad 1 \leq k \leq n, \\ \rho (\delta_t r)^0 - \frac{1}{2} h_t \left(\rho I + \frac{1}{12} h_t^2 L_h\right) \frac{1}{\rho} (a_1^2 r_{11}^0 + \dots + a_n^2 r_{nn}^0) &= \hat{\psi}^0 \quad \text{on } \omega_h, \end{aligned} \quad (3.23)$$

with the approximation errors on the right. The respective boundary and initial data are zero:

$$r|_{\partial\omega_{\mathbf{h}}} = 0, \quad r_{kk}|_{\partial\omega_h} = 0, \quad 1 \leq k \leq n, \quad r^0 = 0.$$

Note that here ψ (with $\psi^0 := 0$), ψ_{kk} and $\hat{\psi}^0$ play the role of $f_{\mathbf{h}}$, b_k and $u_{1\mathbf{h}}$, respectively, in the original scheme equations.

The stability bounds of Theorem 3.1 applied to these equations, together with Remark 3.1 and estimates (3.19), (3.20) and (3.22), lead to the error bound

$$\begin{aligned} &\varepsilon_0 \max_{1 \leq m \leq M} \max \left\{ \underline{\rho}^{1/2} \|\bar{\delta}_t r^m\|_h, \|r^m\|_{E_h}, \|I_{h_t}^m E_h r\|_{I_{\rho\mathbf{h}}} \right\} \\ &\leq (3 + 2\varepsilon_0)(\varepsilon \underline{\rho})^{-1/2} \left[\|\hat{\psi}^0\|_h + h_t \sum_{m=1}^{M-1} \|\psi^m\|_h + \frac{3}{2} a_{\max}^2 h_t \sum_{m=0}^{M-1} (\|\psi_{11}^m\|_h + \dots + \|\psi_{nn}^m\|_h) \right] = \mathcal{O}(|\mathbf{h}|^4). \end{aligned}$$

Using first inequality (3.9) and then $-L_h \leq E_h$ in the last term on the left, we get the error bound (3.21). \square

According to [34], the derived error bound implies the additional error bound for the auxiliary unknowns in weaker “negative” norms. Indeed, from Eqs. (3.23) we get $r_{kk} = s_{kN}^{-1}(\Lambda_k r + \psi_{kk})$ and thus

$$\|(-\Lambda_k)^{-1/2} r_{kk}\|_h \leq \frac{3}{2} (\|(-\Lambda_k)^{1/2} r\|_h + \frac{X_k}{2} \|\psi_{kk}\|_h), \quad 1 \leq k \leq n,$$

see (2.4), that leads to the error bound

$$\sqrt{\varepsilon}\varepsilon_0 \max_{1 \leq k \leq n} \max_{0 \leq m \leq M-1} \|(-\Lambda_k)^{-1/2} (\partial_k^2 u^m - v_{kk}^m)\|_h = \mathcal{O}(|\mathbf{h}|^4).$$

4. Numerical results

This section is devoted to results of our 3D numerical experiments on various tests. The scheme code is written in Pure C language for x64-bit architecture. The figures in this section are plotted with the use of Python standard libraries. The computer with AMD[©] Ryzen[©] 5 7600X 6-Core Processor and 64GB RAM is applied.

First, for $h_1 = \dots = h_n = h$, we consider the error of some scheme in a norm and assume that its convergence rate is some $p > 0$ with respect to both h and h_t :

$$e(h, h_t) = c_1 h^p + c_2 h_t^p,$$

for given data, with $c_1 > 0$ and $c_2 > 0$. Recall that p depends not only on the approximation order of the scheme but on the smoothness order of the data as well, and these orders are the same only for sufficiently smooth data. Then, for some $q > 1$, we get

$$e(h/q, h_t/q) = e(h, h_t)/q^p$$

and, thus, we can find the unknown p due to the well-known Runge-type formula

$$p = p(e) = \ln \frac{e(h, h_t)}{e(h/q, h_t/q)} / \ln q. \quad (4.1)$$

Of course, this practical formula is only approximate. But one can expect that it becomes more and more accurate as h and h_t are chosen smaller and smaller. In Examples 1 and 2, we will analyze the errors $e_{L_h^2}$ in the $H_h = L_h^2$ -norm, $e_{H_h^1}$ in the H_h^1 -norm and $e_{\mathcal{E}_h}$ in the \mathcal{E}_h -norm all taken at the final time moment $t = T$ (unless otherwise is stated). Below we use $q = 5/3$ less than the most common $q = 2$ to cut computational costs in half.

In all the three examples, we choose $a_1 = a_2 = a_3 = a = \text{const}$ even in the case of the variable speed of sound in contrast to [14]. Also we take the cubic domains Ω , i.e., $X_1 = X_2 = X_3 = X$, and the simplest cubic mesh with $N_1 = N_2 = N_3 = N$, i.e., $h_1 = h_2 = h_3 = h = X/N$. As usual, we denote $(x_1, x_2, x_3) = (x, y, z)$.

Example 1. We take $a = 1/\sqrt{3}$, $\Omega = (0, 1)^3$ and $T = 0.3$ as well as the exact travelling wave smooth solution

$$u(x, y, z, t) = \cos(t - x - y - z).$$

The data $f = 0$, u_0 , u_1 and g are taken respectively, and all of them including g are non-zero.

We select values $N = 81, 135, 225, 375$ and $M = 27, 45, 75, 125$ so that the ratio of the consecutive values of both N and M is constant and equals $q = 5/3$. Note that then $\sqrt{3}a(\tau/h) = 0.9 < 1$ ensuring stability of the scheme.

(a) Let first $\rho = 1$ be constant. The results are collected in Table 1, where all the errors are excellent (very small, namely, less than 1.62×10^{-10} even for the least values $N = 81$ and $M = 27$), and the rates $p_{L_h^2}$ are very close to the approximation order 4. The first and second values of the rates $p_{H_h^1}$ and $p_{\mathcal{E}_h}$ are also very close to 4, but their third values become less close to 4 due to the influence of round-off errors. The included theoretical error orders 4.000 hereafter formally correspond to the values $N = M = *$; here all of them equal 4. Notice that, in this and other Tables, always $e_{L_h^2} < e_{\mathcal{E}_h} < e_{H_h^1}$. In this Table, the included value $k = 4$ is the approximation order of the scheme.

(b) Next, we take variable $\rho(x) = 1 + \sin^2 2\pi x \cdot \sin^2 2\pi y \cdot \sin^2 2\pi z$, with $\underline{\rho} = 1$. This does not lead to a significant impact on the results that are put in Table 2. All the results are very close to the corresponding ones in Table 1. For variable ρ , all the errors are even slightly less, but almost all the convergence rates are very slightly less too.

This Table includes the additional column containing the ratio CPU_{rel} of the CPU times for consecutive values of N and M . They are close to the theoretical ratio $(5/3)^4 \approx 7.72$ that is listed last in this column. Note that, for the usual $q = 2$, this ratio is about twice as large: $2^4 = 16$.

Table 1: Example 1(a). Errors $e_{L_h^2}$, $e_{H_h^1}$ and $e_{\mathcal{E}_h}$ and convergence rates $p_{L_h^2}$, $p_{H_h^1}$ and $p_{\mathcal{E}_h}$, for the travelling wave solution and constant ρ

	N	M	$e_{L_h^2}$	$e_{H_h^1}$	$e_{\mathcal{E}_h}$	$p_{L_h^2}$	$p_{H_h^1}$	$p_{\mathcal{E}_h}$
$k = 4$	81	27	2.434899E-11	1.618170E-10	1.166171E-10	—	—	—
	135	45	3.186161E-12	2.119400E-11	1.528949E-11	3.981	3.979	3.977
	225	75	4.153367E-13	2.766222E-12	1.996804E-12	3.989	3.986	3.985
	375	125	5.400149E-14	4.070984E-13	3.056195E-13	3.994	3.751	3.674
	*	*	—	—	—	4.000	4.000	4.000

Table 2: Example 1(b). Errors $e_{L_h^2}$, $e_{H_h^1}$ and $e_{\mathcal{E}_h}$, convergence rates $p_{L_h^2}$, $p_{H_h^1}$ and $p_{\mathcal{E}_h}$ and the ratio of the CPU times for the travelling wave solution and variable ρ

	N	M	$e_{L_h^2}$	$e_{H_h^1}$	$e_{\mathcal{E}_h}$	$p_{L_h^2}$	$p_{H_h^1}$	$p_{\mathcal{E}_h}$	CPU_{rel}
$k = 4$	81	27	2.083224E-11	1.405375E-10	1.035755E-10	—	—	—	—
	135	45	2.725370E-12	1.845130E-11	1.361021E-11	3.982	3.974	3.973	7.40
	225	75	3.552248E-13	2.412085E-12	1.780023E-12	3.989	3.983	3.982	7.49
	375	125	4.618912E-14	3.684124E-13	2.813984E-13	3.993	3.678	3.611	7.87
	*	*	—	—	—	4.000	4.000	4.000	7.72

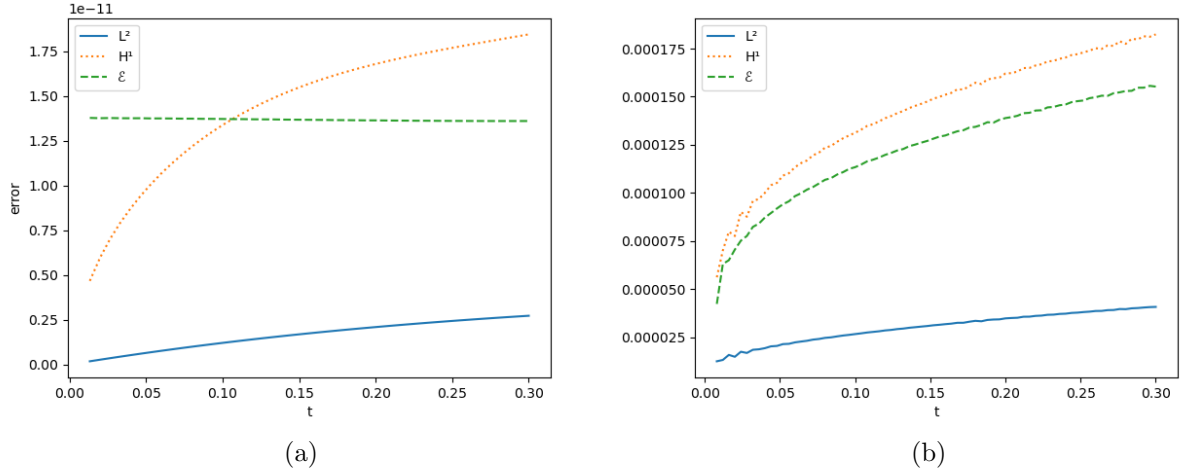


Figure 1: Dynamics of the errors $e_{L_h^2}$, $e_{H_h^1}$ and $e_{\mathcal{E}_h}$ in time for: (a) Example 1(b) for $N = 135$ and $M = 45$, (b) Example 2 in the case $u_1 = w_1$ for $N = 225$ and $M = 75$. In case (b), $100e_{L_h^2}$ is presented instead of $e_{L_h^2}$.

In Fig. 1(a), we also present dynamics of the errors $e_{L_h^2}$, $e_{H_h^1}$ and $e_{\mathcal{E}_h}$ in time. We observe slow and almost linear growth of $e_{L_h^2}$, much more rapid but slower than linear growth of $e_{H_h^1}$ and non-standard very slow linear decrease of $e_{\mathcal{E}_h}$.

Example 2. To analyze the practical error orders for the nonsmooth data, we take the following spherically symmetric initial functions $u_0 = w_1, w_2$, $u_1 = w_0, w_1$ and free term $f = w_0, w_1$ using piecewise

polynomial functions with a finite support in a domain Ω symmetric with respect to the origin:

$$w_0(r) = \begin{cases} 1, & r < r_0 \\ 0, & r > r_0 \end{cases}, \quad w_1(r) = \begin{cases} \frac{r_0 - r}{r_0}, & r \leq r_0 \\ 0, & r > r_0 \end{cases}, \quad w_2(r) = \begin{cases} \left(\frac{r}{r_0}\right)^2 \left(\frac{r_0 - r}{r_0}\right)^2, & r \leq r_0 \\ 0, & r > r_0 \end{cases},$$

with $r = |x|$ and the parameter $r_0 > 0$. Clearly $w_0 \in L^\infty(\mathbb{R}^+)$, $w_1 \in W^{1,\infty}(\mathbb{R}^+)$ and $w_2 \in W^{2,\infty}(\mathbb{R}^+)$, where the usual Lebesgue and Sobolev spaces on $\mathbb{R}^+ = (0, +\infty)$ are used. More importantly below, since w_0, w'_1 and w''_2 are piecewise smooth, we have

$$w_0 \in H^{1/2,2}(\mathbb{R}^+), \quad w_1 \in H^{3/2,2}(\mathbb{R}^+), \quad w_2 \in H^{5/2,2}(\mathbb{R}^+),$$

where now the Nikolskii spaces on \mathbb{R}^+ are invoked, for example, see [2, 22]. So the corresponding smoothness order of w_k is fractional and equals $\lambda = k + 1/2$, for $k = 0, 1, 2$, and namely this is definitive for the convergence rates in the above chosen norms.

Consider a numerical method of the k th approximation order for the IBVP for the wave equation. Below we compare the above 4th order semi-explicit compact scheme and the 2nd order classical explicit scheme

$$\begin{aligned} \rho \Lambda_t v - L_h v &= f \quad \text{on } \omega_h, \\ \rho \delta_t v^0 - \frac{h_t}{2} L_h v^0 &= u_1 + \frac{h_t}{2} f^0 \quad \text{on } \omega_h, \quad v|_{\partial\omega_h} = g, \quad v^0 = u_0 \quad \text{on } \omega_h. \end{aligned}$$

Based on [2, 3, 27], one can expect that, for u_0 of the Nikolskii smoothness order λ and u_1 of the such smoothness order $\lambda - 1$, the errors $e_{L_h^2}$ and $e_{H_h^1}$ together with $e_{\mathcal{E}_h}$ have the convergence rates, respectively,

$$p = \frac{k}{k+1} \lambda, \quad \frac{k}{k+1} (\lambda - 1), \quad \text{for } 0 \leq \lambda \leq k + 1. \quad (4.2)$$

Moreover, $f = w_1$ is independent of t and, thus, its 2nd order Sobolev derivatives $\partial_t^2 f$ and $\partial_t \partial_r f$ are zero and $f = f|_{t=0}$. Therefore, for such f of the Nikolskii smoothness order $\lambda - 2$ in r , one can expect the same convergence rates. Clearly both the rates increase as k grows (and tend to λ and $\lambda - 1$, respectively) that ensures the advantage of higher-order methods over second-order ones not only for smooth data but for nonsmooth data as well, in contrast to the elliptic and parabolic cases. Note that the difference between the two rates (4.2) equals $k/(k+1)$ (i.e., 0.8 for $k = 4$ and 0.666... for $k = 2$) independently on λ .

We recall how to construct the exact spherically symmetric solutions $u(x, t) = u(r, t)$ with $r = |x|$ for the Cauchy problem to the 3D wave equation with the spherically symmetric data. They satisfy the IBVP on the half-line

$$\begin{aligned} \partial_t^2 u &= a^2 \frac{1}{r^2} \partial_r (r^2 \partial_r u) + f(r, t) \quad \text{for } r > 0, \quad t > 0, \\ \partial_r u|_{r=0} &= 0 \quad \text{for } t > 0, \quad u|_{t=0} = u_0(r), \quad \partial_t u|_{t=0} = u_1(r) \quad \text{for } r > 0. \end{aligned}$$

The function $v(r, t) := ru(r, t)$ solves the standard IBVP on the half-line

$$\begin{aligned} \partial_t^2 v &= a^2 \partial_r^2 v + rf(r, t) \quad \text{for } r > 0, \quad t > 0, \\ v|_{r=0} &= 0 \quad \text{for } t > 0, \quad v|_{t=0} = ru_0(r), \quad \partial_t v|_{t=0} = ru_1(r) \quad \text{for } r > 0. \end{aligned}$$

We extend v oddly in r : $v(-r, t) = -v(r, t)$ for $r > 0, t \geq 0$. The extended function v satisfies already the Cauchy problem for the 1D wave equation

$$\begin{aligned} \partial_t^2 v &= a^2 \partial_r^2 v + rf(|r|, t) \quad \text{for } r \in \mathbb{R}, \quad t > 0, \\ v|_{t=0} &= ru_0(|r|), \quad \partial_t v|_{t=0} = ru_1(|r|) \quad \text{for } r \in \mathbb{R} \end{aligned}$$

with the oddly in r extended data u_0, u_1 and f . Thus, u can be represented by the d'Alembert-type formula

$$\begin{aligned} u(r, t) &= \frac{1}{2r} [(r - at)u_0(|r - at|) + (r + at)u_0(|r + at|)] + \frac{1}{2ar} \int_{r-at}^{r+at} qu_1(q) dq \\ &\quad + \frac{1}{2ar} \int_0^t \int_{r-a(t-\tau)}^{r+a(t-\tau)} qf(q, \tau) dq d\tau \quad \text{for } r > 0, \quad t \geq 0. \end{aligned} \quad (4.3)$$

We deal with the following six cases: (a) $u_0 = w_1$; (b) $u_0 = w_2$; (c) $u_1 = w_0$; (d) $u_1 = w_1$; (e) $f = w_0$; (f) $f = w_1$. Here we assume that the data unmentioned in the cases are zero, for example, $u_1 = 0$ and $f = 0$ in case (a). For brevity, we omit the explicit lengthy formulas for $u(r, t)$ in these cases.

We take the symmetric cubic domain $\Omega = (-X/2, X/2)^3$ with $X = 1$ and choose the parameters $a = 1/\sqrt{3}$, $T = 0.3$ and $r_0 = 0.2$. For such parameters, the exact solution is zero at the boundary for all $0 \leq t \leq T$. We take the same values of N and M as above for comparison. Since the values of N are odd, we avoid the formal singularity at $r = 0$ in summands of formula (4.3) when computing u . The numerical solutions in cases (a)-(f) are illustrated in Fig. 2 (visually they do not defer from the exact solutions). As above, we compute the errors $e_{L_h^2}$, $e_{H_h^1}$ and $e_{\mathcal{E}_h}$, the corresponding practical convergence rates $p_{L_h^2}$, $p_{H_h^1}$ and $p_{\mathcal{E}_h}$ according to formula (4.1) as well as the expected theoretical convergence rates according to formulas (4.2) (recall that, in Tables, the last rates are formally attributed to the value $N = M = *$).

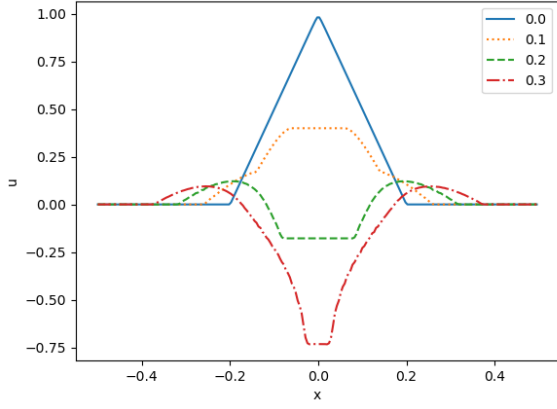
In Tables 3 and 4, we present them for the semi-explicit higher-order scheme ($k = 4$) and classical explicit scheme ($k = 2$) in the cases $u_0 = w_1$ and $u_0 = w_2$, respectively. Hereafter all the errors are many orders of magnitude worse than those for smooth data in Example 1. Also the error $e_{L_h^2}$ is much less (about two orders of magnitude) than $e_{H_h^1}$ and $e_{\mathcal{E}_h}$ compared with Example 1. In Table 3, the errors $e_{H_h^1}$ and $e_{\mathcal{E}_h}$ are rather close to each other. We see the very good agreement between $p_{L_h^2}$ and the corresponding theoretical convergence rates both for $k = 4$ and $k = 2$. The values of $p_{H_h^1}$ and $p_{\mathcal{E}_h}$ are notably less than the theoretical rates, but at least for $k = 4$ they are definitely higher than for $k = 2$. The latter is not surprising since, for low convergence rates, much higher values of N and M are often required to achieve better agreement, even in 1D case, cf. [32]. In Table 4, the errors are about two orders of magnitude less than the corresponding ones in the previous Table, and now we observe the fine agreement between the practical and expected theoretical convergence rates.

Table 3: Example 2(a). Errors $e_{L_h^2}$, $e_{H_h^1}$ and $e_{\mathcal{E}_h}$ and convergence rates $p_{L_h^2}$, $p_{H_h^1}$ and $p_{\mathcal{E}_h}$, for $u_0 = w_1$

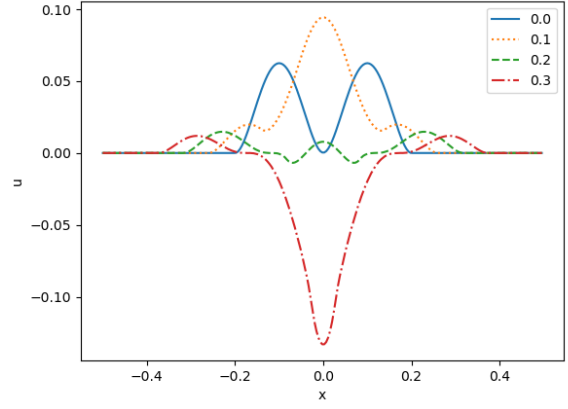
	N	M	$e_{L_h^2}$	$e_{H_h^1}$	$e_{\mathcal{E}_h}$	$p_{L_h^2}$	$p_{H_h^1}$	$p_{\mathcal{E}_h}$
$k = 4$	81	27	4.444064E-4	8.412731E-2	7.300600E-2	—	—	—
	135	45	2.308279E-4	7.058185E-2	6.029682E-2	1.282	0.344	0.374
	225	75	1.208428E-4	5.859705E-2	5.162431E-2	1.267	0.364	0.304
	375	125	6.468215E-5	5.003797E-2	4.327436E-2	1.224	0.309	0.345
	*	*	—	—	—	1.200	0.400	0.400
$k = 2$	81	27	9.032524E-4	1.316278E-1	1.104166E-1	—	—	—
	135	45	5.365153E-4	1.168099E-1	9.645128E-2	1.020	0.234	0.265
	225	75	3.176704E-4	1.016564E-1	8.528642E-2	1.026	0.272	0.241
	375	125	1.899327E-4	8.919430E-2	7.411805E-2	1.007	0.256	0.275
	*	*	—	—	—	1.000	0.333	0.333

Tables 5 and 6 show the results for both the schemes in the cases $u_1 = w_0$ and $u_1 = w_1$, respectively. The agreement between the practical and expected theoretical convergence rates is good for $p_{H_h^1}$ and $p_{\mathcal{E}_h}$ (despite that they are low in Table 5) and not bad for $p_{L_h^2}$. In Table 6, the agreement is better. In addition, Fig. 1(b) shows the dynamics of errors $e_{L_h^2}$, $e_{H_h^1}$ and $e_{\mathcal{E}_h}$ in time in the second case; the error $e_{L_h^2}$ is multiplied by 100 to make its behavior visible. Once again we see a slow and rather close to linear growth of $e_{L_h^2}$. Now both $e_{H_h^1}$ and $e_{\mathcal{E}_h}$ grow much more rapidly but the growth is much slower than linear. Notice oscillations in the behavior of all the errors; their amplitudes diminish in time. Also the amplitudes diminish as N and M grows (in particular, for $N = 81$ and $M = 27$ they are larger; we do not show them).

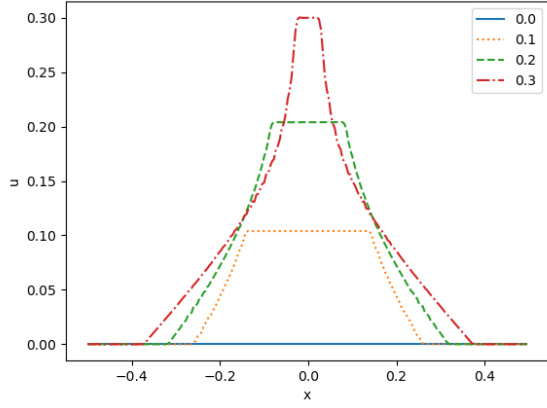
Tables 7 and 8 contain the results concerning the H_h^1 - and \mathcal{E}_h -error norms for the both schemes in the case $f = w_0$ and $f = w_1$, respectively. In Table 7, all the errors are slightly smaller for $k = 4$ than the corresponding ones for $k = 2$. But the practical convergence rates do not differ so significantly and, for the least and other values of N and M , they are closer to the theoretical ones for $k = 4$ and $k = 2$, respectively. In Table 8, the agreement between practical and theoretical convergence rates is nice for $k = 4$ but worse for



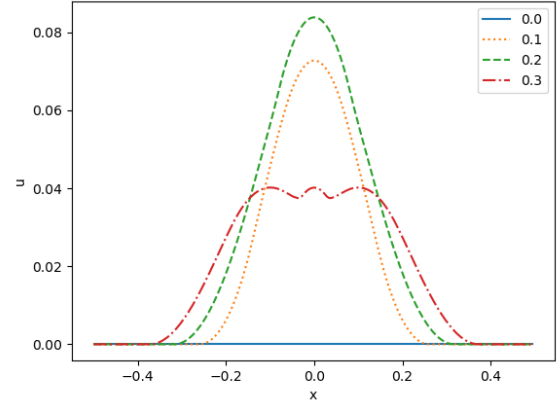
(a)



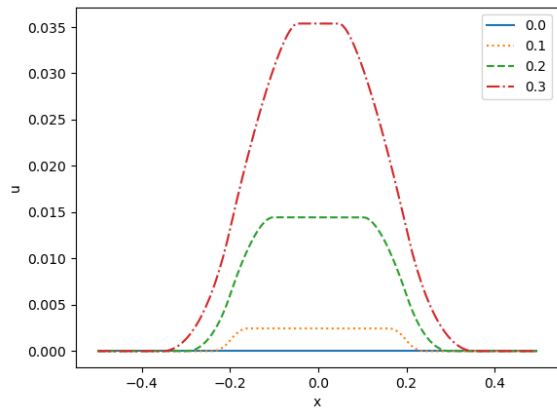
(b)



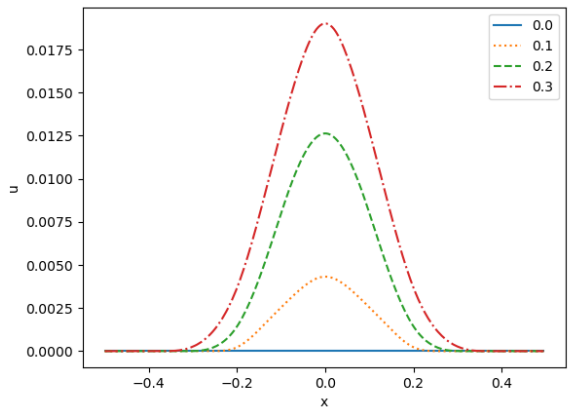
(c)



(d)



(e)



(f)

Figure 2: Example 2. Numerical solutions in the section $y = z = 0$ for $t = 0, 0.1, 0.2$ and 0.3 in the cases: (a) $u_0 = w_1$; (b) $u_0 = w_2$; (c) $u_1 = w_0$; (d) $u_1 = w_1$; (e) $f = w_0$; (f) $f = w_1$.

Table 4: Example 2(b). Errors $e_{L_h^2}$, $e_{H_h^1}$ and $e_{\mathcal{E}_h}$ and convergence rates $p_{L_h^2}$, $p_{H_h^1}$ and $p_{\mathcal{E}_h}$, for $u_0 = w_2$

	N	M	$e_{L_h^2}$	$e_{H_h^1}$	$e_{\mathcal{E}_h}$	$p_{L_h^2}$	$p_{H_h^1}$	$p_{\mathcal{E}_h}$
$k = 4$	81	27	1.801824E-5	3.162480E-3	2.714343E-3	—	—	—
	135	45	6.263696E-6	1.740913E-3	1.519010E-3	2.068	1.169	1.136
	225	75	2.200167E-6	9.725291E-4	8.279443E-4	2.048	1.140	1.188
	375	125	7.757714E-7	5.362174E-4	4.555987E-4	2.041	1.165	1.169
	*	*	—	—	—	2.000	1.200	1.200
$k = 2$	81	27	7.455862E-5	7.888876E-3	6.577538E-3	—	—	—
	135	45	3.209740E-5	4.835505E-3	4.021807E-3	1.650	0.9582	0.9630
	225	75	1.379373E-5	2.964015E-3	2.440001E-3	1.653	0.9581	0.9783
	375	125	5.918562E-6	1.804674E-3	1.482635E-3	1.656	0.9713	0.9752
	*	*	—	—	—	1.667	1.0000	1.0000

Table 5: Example 2(c). Errors $e_{L_h^2}$, $e_{H_h^1}$ and $e_{\mathcal{E}_h}$ and convergence rates $p_{L_h^2}$, $p_{H_h^1}$ and $p_{\mathcal{E}_h}$, for $u_1 = w_0$

	N	M	$e_{L_h^2}$	$e_{H_h^1}$	$e_{\mathcal{E}_h}$	$p_{L_h^2}$	$p_{H_h^1}$	$p_{\mathcal{E}_h}$
$k = 4$	81	27	2.173270E-4	3.947877E-2	3.380764E-2	—	—	—
	135	45	1.325706E-4	3.207199E-2	2.725321E-2	0.968	0.407	0.422
	225	75	6.682470E-5	2.591038E-2	2.247714E-2	1.341	0.418	0.377
	375	125	3.317065E-5	2.138626E-2	1.834409E-2	1.371	0.376	0.397
	*	*	—	—	—	1.200	0.400	0.400
$k = 2$	81	27	3.542877E-4	5.359390E-2	4.470650E-2	—	—	—
	135	45	2.165218E-4	4.603917E-2	3.790000E-2	0.964	0.297	0.323
	225	75	1.233063E-4	3.924349E-2	3.274401E-2	1.102	0.313	0.286
	375	125	7.091202E-5	3.370893E-2	2.793154E-2	1.083	0.298	0.311
	*	*	—	—	—	1.000	0.333	0.333

$k = 2$, but the practical rates for $k = 4$ are definitely larger than for $k = 2$. In the both cases, the behavior of $e_{L_h^2}$ and $p_{L_h^2}$ seems still rather chaotic, and we omit them.

Finally, in all the cases, we observe the advantages in error behavior of the semi-explicit higher order scheme over the standard explicit scheme.

Example 3. This example is similar to a part of Example 6 in [31], where one computes the wave propagation in the three-layer medium in x , with the different speeds of sound 1.5, 1 and 3 km/sec, respectively, in its left, middle and right layers of the domain $\Omega = (0, X)^3$ with $X = 3$ km. The layers have the same thickness 1 km. Recall that, in these layers, we set $a = 1$ but take $\rho = 4/9, 1$ and $1/9$ (sec/km)², respectively. The source is the Ricker-type wavelet (popular in geophysics) smoothed in space

$$f(x, y, z, t) = \varphi_\gamma(r)\psi(t), \quad \text{with} \quad \varphi_\gamma(r) = \left(\frac{\pi}{\gamma}\right)^{3/2} e^{-\gamma r^2}, \quad \int_{\mathbb{R}^3} \varphi_\gamma(r) dx dy dz = 1, \quad \psi(t) = \sin(50t)e^{-200t^2},$$

where now $r = |(x - x_0, y - y_0, z - z_0)|$, $(x_0, y_0, z_0) = (1.5, 1.5, 1.5)$ is the center of domain, and $\gamma \gg 1$ is a parameter. Also we take $u_0 = u_1 = 0$, $\gamma = 10000$ and $T = 0.8$ sec. The multipliers $\varphi_\gamma(r)$ and $\psi(t)$ are plotted in Fig. 3.

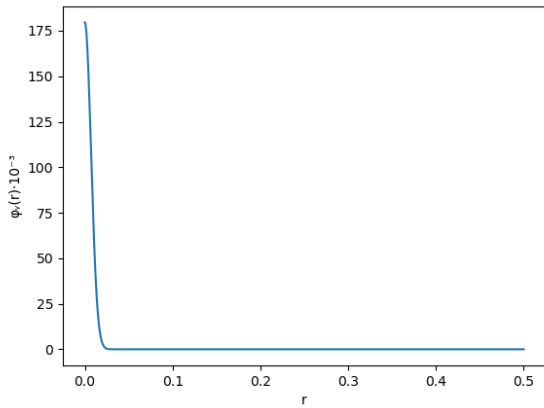
We present figures similar to those given in [31]. The results are in general close to those from [31] where $\varphi_\gamma(r)$ was taken as the delta-function concentrated at (x_0, y_0, z_0) , but with some essential differences that we discuss below. In Fig. 4, we demonstrate the 2D wave fields in section $z = 1.5$ computed for $N = 400$ and $M = 560$ (i.e., $h = 0.0075$ and $h_t = 1/700$) at six time moments. In Fig. 4(a) and (b), the spherical wave is

Table 6: Example 2(d). Errors $e_{L_h^2}$, $e_{H_h^1}$ and $e_{\mathcal{E}_h}$ and convergence rates $p_{L_h^2}$, $p_{H_h^1}$ and $p_{\mathcal{E}_h}$, for $u_1 = w_1$

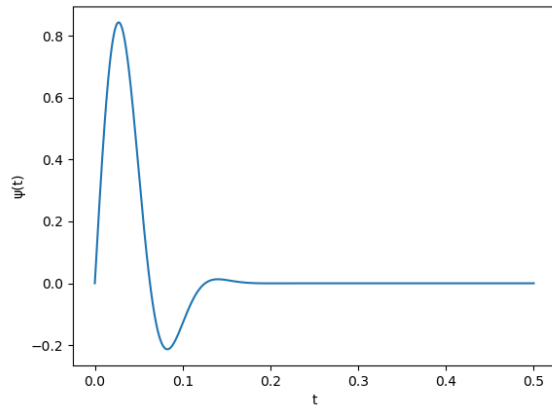
	N	M	$e_{L_h^2}$	$e_{H_h^1}$	$e_{\mathcal{E}_h}$	$p_{L_h^2}$	$p_{H_h^1}$	$p_{\mathcal{E}_h}$
$k = 4$	81	27	3.486452E-6	6.014188E-4	5.177318E-4	—	—	—
	135	45	1.201817E-6	3.370573E-4	2.921310E-4	2.085	1.134	1.120
	225	75	4.077593E-7	1.824089E-4	1.552747E-4	2.116	1.202	1.237
	375	125	1.412191E-7	9.888468E-5	8.401369E-5	2.076	1.199	1.202
	*	*	—	—	—	2.000	1.200	1.200
$k = 2$	81	27	1.585246E-5	1.435502E-3	1.178713E-3	—	—	—
	135	45	6.463676E-6	8.736566E-4	7.217399E-4	1.756	0.9721	0.9602
	225	75	2.666898E-6	5.271610E-4	4.330681E-4	1.733	0.9890	0.9999
	375	125	1.110063E-6	3.184605E-4	2.613995E-4	1.716	0.9867	0.9883
	*	*	—	—	—	1.667	1.0000	1.0000

Table 7: Example 2(e). Errors $e_{H_h^1}$ and $e_{\mathcal{E}_h}$ and convergence rates $p_{H_h^1}$ and $p_{\mathcal{E}_h}$, for $f = w_0$

	N	M	$e_{H_h^1}$	$e_{\mathcal{E}_h}$	$p_{H_h^1}$	$p_{\mathcal{E}_h}$
$k = 4$	81	27	8.346416E-4	5.933564E-4	—	—
	135	45	4.141449E-4	3.080528E-4	1.371	1.283
	225	75	2.412233E-4	1.795166E-4	1.058	1.057
	375	125	1.451002E-4	1.071878E-4	0.995	1.010
	*	*	—	—	1.200	1.200
$k = 2$	81	27	9.056331E-4	6.841736E-4	—	—
	135	45	4.786699E-4	3.766503E-4	1.248	1.168
	225	75	2.718633E-4	2.150001E-4	1.107	1.098
	375	125	1.586915E-4	1.253125E-4	1.054	1.057
	*	*	—	—	1.000	1.000



(a)



(b)

Figure 3: Example 3. Multipliers $\varphi_\gamma(r)$ for $\gamma = 10000$ and $\psi(t)$ of the source function.

Table 8: Example 2(f). Errors $e_{H_h^1}$ and $e_{\mathcal{E}_h}$ and convergence rates $p_{H_h^1}$ and $p_{\mathcal{E}_h}$, for $f = w_1$

	N	M	$e_{H_h^1}$	$e_{\mathcal{E}_h}$	$p_{H_h^1}$	$p_{\mathcal{E}_h}$
$k = 4$	81	27	5.459770E-6	4.493218E-6	—	—
	135	45	1.857594E-6	1.523632E-6	2.111	2.117
	225	75	6.319904E-7	5.259791E-7	2.111	2.082
	375	125	2.205933E-7	1.838900E-7	2.060	2.057
	*	*	—	—	2.000	2.000
$k = 2$	81	27	4.351183E-5	3.003301E-5	—	—
	135	45	1.676865E-5	1.173838E-5	1.867	1.839
	225	75	6.422439E-6	4.604730E-6	1.879	1.832
	375	125	2.507550E-6	1.836635E-6	1.841	1.799
	*	*	—	—	1.666	1.666

expanding inside the middle layer and leaving the enlarging neighborhood of the center of the domain. In Fig. 4(c), the wave reaches the boundaries between the layers and only begins to penetrate into the right layer. In Fig. 4(d), the penetration to the left and right layers together with reflections from the boundaries of these layers inside the middle layer are already visible well. Both the effects are stronger for the right layer with the maximal speed of sound. In Fig. 4(e) and (f), both the penetrations and reflections evolve rapidly and, in the last figure, the wave front almost approaches the right boundary of the domain.

We supplement the last figure by Fig. 5 and 6 showing the 1D dynamics of the wave at different times for $y = z = 1.5$ and $x = z = 1.5$, respectively, at five (from above six) time moments. These figures are nonsymmetric in x and symmetric in y , respectively, as it should be. Of course, this dynamics corresponds to those shown in the previous figure in the perpendicular directions $x = 1.5$ and $z = 1.5$, respectively, but it also contains additional information about the amplitude and form of the moving wave fronts. The results are given for $N = 200$ as in [31] and $N = 400$ as above, respectively. In general, they are close, but the results for $N = 200$ suffer from parasitic numerical oscillations. Unfortunately, the results in [31] (including the counterparts of Fig. 4(e) and (f)) also contain such parasitic oscillations essentially distorting the exact solution in some subdomains where it is rather small.

We also make a note on the quality of contour levels. Fig. 4 is plotted via the *matplotlib.pyplot* library for Python 3.10.9. It is crucial to choose properly its parameter *levels* defining the maximal amount of levels in use. For $N = 400$ and small values of *levels* like 14, we encountered false visible oscillations and the false observation of the wave achieving the right boundary of the domain, without its reflection. Setting that parameter like N provided us with correct results.

Acknowledgements

The work was supported by the Russian Science Foundation, grant no. 23-21-00061.

Declaration of competing interest

The authors have no conflicts of interest to declare that are relevant to the content of this paper.

References

- [1] G.A. Baker, J.H. Bramble, Semidiscrete and single step fully discrete approximations for second order hyperbolic equations, *RAIRO. Anal. Numér.* 13 (1979) 75–1000. <https://doi.org/10.2307/2008283>
- [2] J. Bergh, J. Löfström. *Interpolation Spaces. An Introduction*, Springer, Berlin–New York, 1976.
- [3] P. Brenner, V. Thomée, L.B. Wahlbin. *Besov Spaces and Applications to Difference Methods for Initial Value Problems*. Springer, Berlin, 1975.

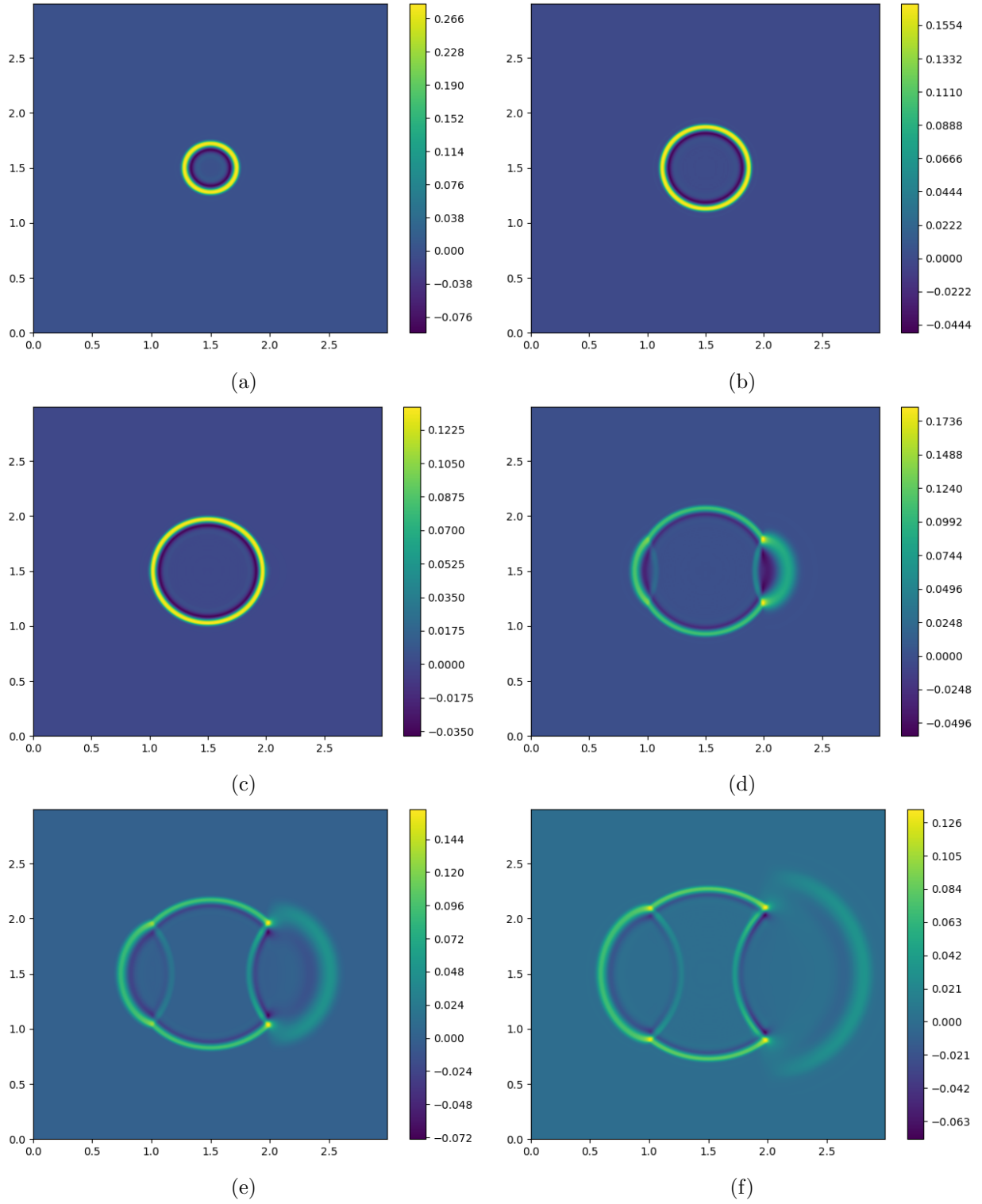


Figure 4: Example 3. Contour levels of wavefields in section $z = 1.5$ computed for $h = 0.075$ and $h_t = 1/700$ at: (a) $t = 0.25$; (b) $t = 0.4$; (c) $t = 0.5$; (d) $t = 0.6$; (e) $t = 0.7$; (f) $t = 0.8$.

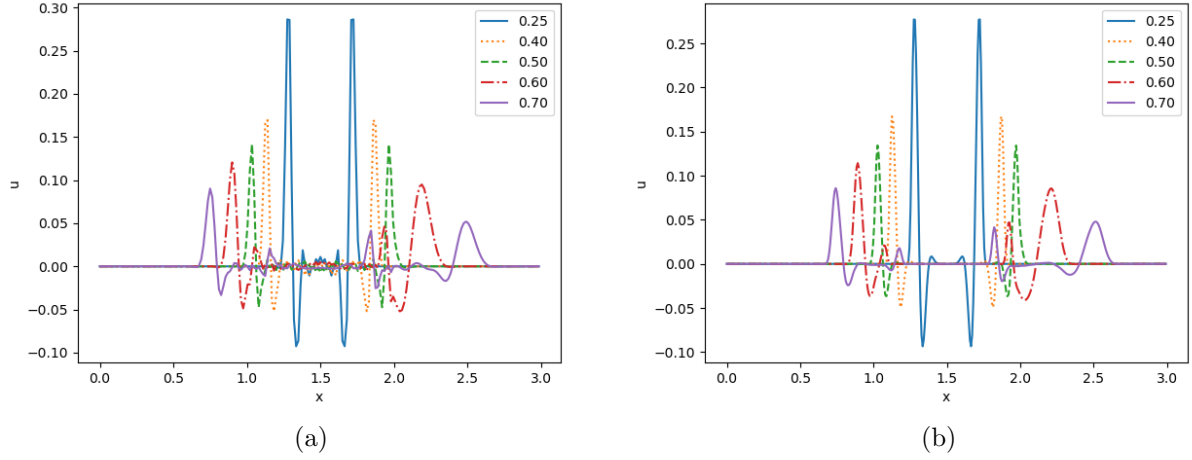


Figure 5: Example 3. Dynamics of the waves at different times for $y = z = 1.5$: (a) $h = 0.015$, $h_t = 1/352$ for $t = 0.25$ and $h_t = 1/350$ for other times; (b) $h = 0.075$ and $h_t = 1/700$.

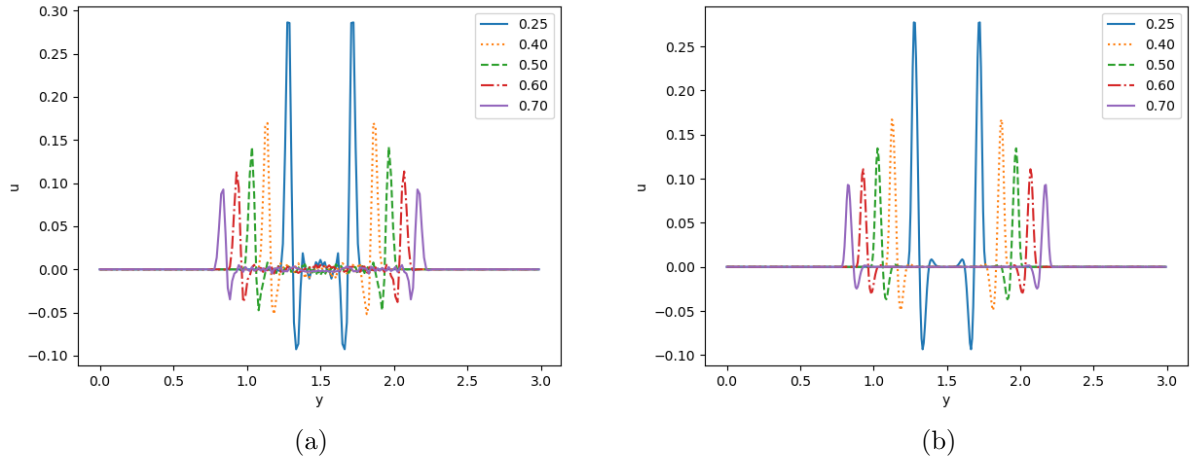


Figure 6: Example 3. Dynamics of the waves at different times for $x = z = 1.5$: (a) $h = 0.015$, $h_t = 1/352$ for $t = 0.25$ and $h_t = 1/350$ for other times; (b) $h = 0.0075$ and $h_t = 1/700$.

- [4] S. Britt, E. Turkel, S. Tsynkov, A high order compact time/space finite difference scheme for the wave equation with variable speed of sound, *J. Sci. Comput.* 76(2) (2018) 777–811. <https://doi.org/10.1007/s10915-017-0639-9>.
- [5] E. Burman, O. Duran, A. Ern, Hybrid high-order methods for the acoustic wave equation in the time domain, *Commun. Appl. Math. Comput.* 4(2) (2022) 597–633. <https://doi.org/10.1007/s42967-021-00131-8>
- [6] J. Chabassier, J. Diaz, S. Imperiale, Construction and analysis of fourth order, energy consistent, family of explicit time discretizations for dissipative linear wave equations, *ESAIM: Math. Model. Numer. Anal.* 54(3) (2020) 845–878. <https://doi.org/10.1051/m2an/2019079>.
- [7] M. Ciment, S.H. Leventhal, Higher order compact implicit schemes for wave equation, *Math. Comput.* 29(132) (1975) 985–994.
- [8] B. Cockburn, Z. Fu, A. Hungria, L. Ji, M.A. Sánchez, F.-J. Sayas, Stormer-Numerov HDG methods for acoustic waves, *J. Sci. Comput.* 75 (2018) 597–624. <https://doi.org/10.1007/s10915-017-0547-z>.
- [9] G.C. Cohen, *Higher-Order Numerical Methods for Transient Wave Equations*. Springer, Berlin, 2002.
- [10] D. Deng, C. Zhang, Application of a fourth-order compact ADI method to solve a two-dimensional linear hyperbolic equation, *Int. J. Comput. Math.* 90(2) (2013) 273–291. <https://doi.org/10.1080/00207160.2012.713475>.
- [11] D. Deng, C. Zhang, Analysis of a fourth-order compact ADI method for a linear hyperbolic equation with three spatial

- variables, *Numer. Algorithms* 63 (2013) 1–26. <https://doi.org/10.1007/s11075-012-9604-8>
- [12] V.I. Fedorchuk, On the invariant solutions of some five-dimensional d'Alembert equations, *J. Math. Sci.* 220(1) (2017) 27–37. <https://doi.org/10.1007/s10958-016-3165-7>
- [13] Y. Jiang, Y. Ge, An explicit fourth-order compact difference scheme for solving the 2D wave equation, *Adv. Difference Equat.* 415 (2020) 1–14. <https://doi.org/10.1186/s13662-020-02870-z>
- [14] Y. Jiang, Y. Ge, An explicit high-order compact difference scheme for the three-dimensional acoustic wave equation with variable speed of sound, *Int. J. Comput. Math.* 100(2) (2023) 321–341. <https://doi.org/10.1080/00207160.2022.2118524>
- [15] B. Hou, D. Liang, H. Zhu, The conservative time high-order AVF compact finite difference schemes for two-dimensional variable coefficient acoustic wave equations, *J. Sci. Comput.* 80 (2019) 1279–1309. <https://doi.org/10.1007/s10915-019-00983-6>
- [16] K. Li, W. Liao, Y. Lin, A compact high order alternating direction implicit method for three-dimensional acoustic wave equation with variable coefficient, *J. Comput. Appl. Math.* 361(1) (2019) 113–129. <https://doi.org/10.1016/j.cam.2019.04.013>
- [17] H.-L. Liao, Z.-Z. Sun, A two-level compact ADI method for solving second-order wave equations, *Int. J. Comput. Math.* 90(7) (2013) 1471–1488. <http://dx.doi.org/10.1080/00207160.2012.754016>
- [18] W. Liao, On the dispersion and accuracy of a compact higher-order difference scheme for 3D acoustic wave equation, *J. Comput. Appl. Math.* 270 (2014) 571–583. <https://doi.org/10.1016/j.cam.2013.08.024>
- [19] W. Liao, P. Yong, H. Dastour, J. Huang, Efficient and accurate numerical simulation of acoustic wave propagation in a 2D heterogeneous media, *Appl. Math. Comput.*, 321 (2018) 385–400. <https://doi.org/10.1016/j.amc.2017.10.052>
- [20] G.I. Marchuk, Splitting and alternating direction methods, in *Handbook of Numerical Analysis, Finite Difference Methods – Solution of Equations in R^n (Part 1)*, P.G. Ciarlet and J.L. Lions, eds., Elsevier, Amsterdam, 203–462, 1990. [https://doi.org/10.1016/S1570-8659\(05\)80035-3](https://doi.org/10.1016/S1570-8659(05)80035-3)
- [21] P.P. Matus, H.T.K. Anh, Compact difference schemes for the multidimensional Klein-Gordon equation, *Diff. Equat.* 58(1) (2022) 120–138. <https://doi.org/10.1134/S0012266122010128>
- [22] S.M. Nikol'skii, *Approximation of Functions of Several Variables and Imbedding Theorems*, Springer, Berlin-Heidelberg, 1975.
- [23] V. Paasonen, Compact schemes for systems of second-order equations without mixed derivatives, *Russ. J. Numer. Anal. Math. Model.* 13(4), 335–344 (1998). <https://doi.org/10.1515/rnam.1998.13.4.335>
- [24] S. Schoeder, K. Kormann, W.A. Wall, M. Kronbichler, Efficient explicit time stepping of high order discontinuous Galerkin schemes for waves, *SIAM J. Sci. Comput.* 40(6) (2018) C803–C826. <https://doi.org/10.1137/18M1185399>
- [25] F. Smith, S. Tsynkov, E. Turkel, Compact high order accurate schemes for the three dimensional wave equation, *J. Sci. Comput.* 81(3) (2019) 1181–1209. <https://doi.org/10.1007/s10915-019-00970-x>
- [26] W. Zhang, L. Tong, E.T. Chung, A new high accuracy locally one-dimensional scheme for the wave equation, *J. Comput. Appl. Math.* 236(6) (2011) 1343–1353. <https://doi.org/10.1016/j.cam.2011.08.022>
- [27] A.A. Zlotnik, Convergence rate estimates of finite-element methods for second order hyperbolic equations, in *Numerical Methods and Applications*, G.I. Marchuk, ed., CRC Press, Boca Raton, 155–220, 1994.
- [28] A. Zlotnik, On properties of an explicit in time fourth-order vector compact scheme for the multidimensional wave equation, Preprint (2021) 1–15. <https://arxiv.org/abs/2105.07206>
- [29] A.A. Zlotnik, B.N. Chetverushkin, Stability of numerical methods for solving second-order hyperbolic equations with a small parameter, *Dokl. Math.* 101(1) (2020) 30–35. <https://doi.org/10.1134/S1064562420010226>
- [30] A. Zlotnik, R. Čiegis, On higher-order compact ADI schemes for the variable coefficient wave equation, *Appl. Math. Comput.* 412 (2022) article 126565. <https://doi.org/10.1016/j.amc.2021.126565>
- [31] A. Zlotnik, R. Čiegis, On construction and properties of compact 4th order finite-difference schemes for the variable coefficient wave equation, *J. Sci. Comput.* 95(1) (2023) article 3. <https://doi.org/10.1007/s10915-023-02127-3>
- [32] A. Zlotnik, O. Kireeva, Practical error analysis for the bilinear FEM and finite-difference scheme for the 1D wave equation with nonsmooth data, *Math. Model. Anal.* 23(3) (2018) 359–378. <https://doi.org/10.3846/mma.2018.022>
- [33] A. Zlotnik, O. Kireeva, On compact 4th order finite-difference schemes for the wave equation, *Math. Model. Anal.* 26(3) (2021) 479–502. <https://doi.org/10.3846/mma.2021.13770>
- [34] A. Zlotnik, T. Lomonosov, On stability and error bounds of an explicit in time higher-order vector compact scheme for the multidimensional wave and acoustic wave equations, *Appl. Numer. Math.* 195 (2024) 54–74. <https://doi.org/10.1016/j.apnum.2023.09.006>